A Molecular View on the Interaction of the Trojan Peptide Penetratin with the Polar Interface of Lipid Bilayers

Hans Binder and Göran Lindblom
Department of Biophysical Chemistry, Umeå University, Umeå, Sweden

ABSTRACT Penetratin belongs to the family of Trojan peptides that effectively enter cells and therefore can be used as cargos for agents that are unable to penetrate the cell membrane. We applied polarized infrared spectroscopy in combination with the attenuated total reflection technique to extract information before penetratin binding to lipid membranes with molecular resolution. The amide I band of penetratin in the presence of zwitterionic dimyristoylphosphatidylcholine and of anionic lipid membranes composed of dioleoylphosphatidylcholine and dioleoylphosphatidylglycerol shows the characteristics of an antiparallel β-sheet with a small fraction of turns. Both signatures have been interpreted in terms of a hairpin conformation. The infrared linear dichroism of the amide I band indicates that the peptide chain orients in an oblique fashion whereas the plane of the sheet aligns virtually parallel with respect to the membrane surface. The weak effect of the peptide on dimyristoylphosphatidylcholine gives indication of its superficial binding where the charged lysine and arginine side chains form H-bonds to the phosphate oxygens of the surrounding lipids. The determinants for internalization of penetratin appear to be a peptide sequence with a distribution of positively charged residues along a β-sheet conformation, which enables the anchoring of the peptide in the polar part of the membranes and the effective compensation of anionic lipid charges.

INTRODUCTION

Trojan peptides are able to translocate into cells without deleterious effects. In addition, they are capable of carrying covalently associated cargo molecules such as short peptides, larger functional enzymes, and even polynucleotide sequences (Pooga et al., 1998; Prochiantz, 1996). This phenomenon has opened up the possibility of the routine modulation of specific signaling pathways in cells or even tissues by the rational design of signaling modulators coupled to these internalizing sequences. Penetratin, also known as pAntp peptide, was the first member of this rapidly expanding family of peptide-based cellular transporters originating from either natural or synthetic sources. For example, polycationic homopolymers such as short oligomers of arginine effectively enter cells and, in addition, these peptides can be used to enable or enhance uptake of agents into cells that do not enter or do so only poorly in unconjugated form (Mitchell et al., 2000; Rothbard et al., 2002).

Penetratin and other Trojan peptides do not belong to the amphipathic helical peptide family, whose members are able to translocate membranes by pore formation or by a detergent-like mechanism (Ladokhin and White, 2001). It was shown experimentally and by molecular modeling that penetratin is not sufficiently hydrophobic to insert deeply into the phospholipid model membranes (Drin et al., 2001a). Instead, this peptide preferentially remains at the interface between the phospholipid bilayer and the aqueous environment (Fragneto et al., 2000).

In our previous publications we used isothermal titration calorimetry to get a better understanding of factors that affect the peptide binding to lipid membranes and its permeation through the bilayer (Binder and Lindblom, 2003a). The results were interpreted in terms of an electroporation-like mechanism according to which the asymmetrical distribution of the peptide between the outer and inner surfaces of charged bilayers causes a transmembrane electrical field that alters the lateral and curvature stresses within the membrane. At a threshold value these effects induce internalization of penetratin. Both the cationic charge of the peptide and the anionic charge of the membrane are essential for the ability of Trojan peptides to translocate across lipid bilayers.

These results clearly indicate that electrostatics play a key role for penetratin binding and internalization. The experimental data were interpreted in terms of the surface partitioning model, which assumes that electrostatic interactions cause an enrichment of cationic peptide in the aqueous phase near the anionic membrane interface and in this way facilitates binding of the peptide to the membrane. Association of penetratin with the lipid bilayers is essentially driven by an enthalpy gain of $-$(20–30) kJ/mole (Binder and Lindblom, 2003b). It has been suggested that the change of enthalpy results from the nonclassical hydrophobic effect (i.e., specific interactions between the lipid and the peptide and/or a strengthening of lipid-lipid interactions) and a membrane-induced conformational change of penetratin from a disordered into an α-helical and/or β-sheet structure. Hence, a charge-independent affinity of the peptide to lipid membranes seems to play an important role that affects the translocation of cargo peptides across lipid membranes. The

Submitted August 31, 2003, and accepted for publication February 3, 2004.

Address reprint requests to Hans Binder at his present address: Interdisciplinary Centre for Bioinformatics of Leipzig University, Kreuzstr. 7b, D-4103 Leipzig, Germany. Fax: 49-341-1495-119; E-mail: binder@rz.uni-leipzig.de.

0006-3495/04/07/332/12 $2.00

doi: 10.1529/biophysj.103.034025

lipid-induced change of the secondary structure of penetratin possibly affects its hydrophobicity, and thus its insertion mode as well, before internalization. Such structural details are unknown at present.

A number of spectroscopic studies have been published with the purpose of determining the structure of penetratin both in solution and upon binding to lipid bilayers (Christiaens et al., 2002; Derossi et al., 1994; Drin et al., 2001a; Hällbrink et al., 2001; Lindgren et al., 2000; Magzoub et al., 2002, 2001; Persson et al., 2003, 2001; Salamon et al., 2003; Thoren et al., 2000). In membrane mimetic environments such as trifluorethanol (Czajlik et al., 2002) and sodium dodecylsulphate micellar solution (Berlose et al., 1996; Drin et al., 2001a; Lindberg and Gräslund, 2001), the peptide seems to adopt a helical structure. An α-helical conformation was also reported for penetratin which is bound to lipid membranes (Persson et al., 2001). However, the helical-wheel projection of penetratin reveals that the seven cationic residues almost evenly distribute over the surface of the α-helix (see Fig. 1 in Drin et al., 2001b), and thus the question of how a helix incorporates into an apolar environment such as the hydrophobic core of the bilayer remains open. Other authors found that helix formation does not seem to be a prerequisite for lipid binding or for cell internalization of penetratin (Derossi et al., 1996).

Infrared reflection absorption spectroscopy on mixed penetratin-lipid monolayers at the water/air interface shows that the secondary structure of the peptide is dominated by an antiparallel β-sheet, especially in the presence of charged lipids in contrast to the α-helical conformation within the native *Antennapedia* homeodomain (Bellet-Amalric et al., 2000). The authors propose a hairpin-like structure, which adopts an oblique orientation with respect to the membrane plane. These results were confirmed by Magzoub and coworkers, who found, by circular dichroism spectroscopy, that penetratin predominantly adopts a β-sheet conformation in the presence of lipid vesicles and a random coil structure in solution (Magzoub et al., 2002, 2001). The latter data, however, suggest that the situation might be more complex, since a significant helical content was also detected at low penetratin concentrations. The authors conclude that penetratin, when residing at the surface of a membrane, is chameleon-like in its induced structure.

In this publication we used infrared (IR) dichroism spectroscopy in combination with the technique of attenuated total reflection (ATR) which have been proven to provide a detailed molecular view on orientations, conformations, and interactions in lipid membranes (Binder, 2003). The work is aimed to extract information about the secondary structure of membrane bound penetratin, its orientation with respect to the membrane surface and peptide-induced perturbations of the architecture of the lipid bilayer and of the hydration of its polar interface. Lipid multibilayer stacks are studied in the fully hydrated state and at reduced hydration to get insights into details of water lipid interactions in the presence of the peptide. We focus on lipid/peptide molar ratios that are comparable with the relevant concentration of membrane bound peptide at which the peptide translocates through the bilayer (Binder and Lindblom, 2003a). This choice was motivated by obtaining a better understanding of structural factors that might be related to the translocation mechanism of the peptide.

MATERIALS AND METHODS

Materials

Penetratin (Arg-Gln-Ile-Lys-Ile-Trp-Phe-Gln-Asn-Arg-Arg-Met-Lys-Trp-Lys-Lys), was solid-phase-synthesized by Dr. A. Engstrom at the University of Uppsala (Sweden). The zwitterionic, neutral phospholipids dimyristoylphosphatidylcholine (DMPC) and dioleoylphosphatidylcholine (DOPC) and the anionic phospholipid dioleoylphosphatidylglycerol (DOPG) were purchased from Avanti Polar Lipids (Alabaster, AL). Penetratin and the lipids were weighed and directly dissolved in definite amounts of organic solvent (chloroform:methanol; 3:1 v/v) to give stock solutions (2–5 mM), which were then mixed to provide the desired composition in terms of lipid/peptide molar ratio (L/P), and of DOPC/DOPG in terms of the molar fraction of DOPG, X_{PG}.

Infrared linear dichroism measurements

Lipid films were prepared by pipetting 100–200 μl of the sample solution on a ZnSe attenuated total reflection (ATR) crystal ($70 \times 10 \times 5$ mm^3 trapezoid, face angle 45°, six active reflections) and evaporating the solvent under a stream of warm air. While drying, the material was spread uniformly over an area of $A_{film} \approx 40 \times 7$ mm^2 onto the crystal surface by gently stroking with the pipette tip. The amount of material corresponds to an average thickness of the dry film >3 μm, assuming a density of 1 g/cm^3.

The ATR crystal was mounted into a commercial horizontal ATR holder (Graseby Specac, Kent, UK) that had been modified such as to realize a well-defined relative humidity (RH) and temperature (T) within the sample chamber (Binder et al., 1997). We used a flowing water thermostat (Julabo, Seelbach, Germany) and a moisture generator (HumiVar, Leipzig, Germany) to adjust RH (D_2O) to any value between 5% and 98%, with an accuracy of $\pm$0.5%. For a second line of measurements under excess water conditions the film was hydrated using a wet sponge placed within the sealed sample chamber. The samples were equilibrated in a saturated atmosphere of D_2O vapor for at least several hours before starting the IR measurements. Note that these conditions ensure a relative humidity of $RH = 100\%$ and thus full hydration of the sample.

Polarized absorbance spectra, $A_{\parallel}(\nu)$ and $A_{\perp}(\nu)$ (128 scans, nominal resolution 2 cm^{-1}), were recorded by means of a BioRad FTS-60a Fourier transform infrared spectrometer (Digilab, Randolph, MA) at two perpendicular polarizations of the IR beam, parallel ($\parallel$) and perpendicular ($\perp$) with respect to the plane of incidence.

The dichroic ratio of an absorption band, $R = A_{\parallel}/A_{\perp}$, provides the infrared order parameter of the respective transition moment, $\boldsymbol{\mu}$, relative to the optical axis given by the membrane normal, $\mathbf{n}$,

$$S_{IR} \equiv 0.5 < 3 \times \cos^2 \theta_{\mu n} - 1 > = (R-2)(R+2.55) \quad (1)$$

(see Harrick, 1967, and Binder, 2003, and references cited therein).

The molecular ordering of the hydrocarbon chains can be quantified by means of the longitudinal chain order parameter using the IR order parameters of the symmetric and antisymmetric CH_2 stretching bands, $S_{IR}(\nu_s)$ and $S_{IR}(\nu_{as})$, respectively (Binder and Gawrisch, 2001; Binder and Schmiedel, 1999):

$$S_\theta = -(S_{IR}(\nu_s) + S_{IR}(\nu_{as})). \quad (2)$$

It gives a measure of the mean segmental order and of the mean tilt of the chain axes with respect to the bilayer normal.

The spectrum of the dichroic ratio is defined as

$$R(\nu) \equiv A_\parallel(\nu)/A_\perp(\nu). \quad (3)$$

It provides an estimation of the orientation of the transition moments within a given spectral range. Moreover, $R(\nu)$ helps to improve the spectral resolution in the range of overlapping bands referring to differently oriented transition moments.

The peak positions and the center of gravity (COG) of the absorption bands were determined from the weighted sum spectrum $A(\nu) = A_\parallel(\nu) + 2.55\ A_\perp(\nu)$ referring to the absorbance of nonpolarized radiation (Binder, 2003; Binder and Schmiedel, 1999).

RESULTS AND DISCUSSION

The effect of penetratin on the phase behavior of DMPC

Fig. 1 shows the center of gravity of the symmetric methylene stretching band, $\nu_s(CH_2)$, of pure DMPC and of DMPC in the presence of penetratin (molar ratio, $(L/P) = 30$) in a saturated D_2O vapor atmosphere as a function of temperature. The sigmoidal increase in $\nu_s(CH_2)$ reflects the main phase transition of the lipid. The inflection point marks the transition temperature of the DMPC multibilayer stacks at 24.5°C, which agrees with the transition temperature of fully hydrated DMPC multilamellar vesicles that was measured using differential scanning calorimetry (DSC, see below). The transition temperature of the DMPC+penetratin system is downwards shifted by ~1 K compared with pure DMPC. In addition, the mean band position of the methylene stretches, $\nu_s(CH_2)$, systematically shifts toward higher wavenumbers after addition of the peptide. This tendency was observed in repeated measurements of independently prepared samples. It can be tentatively explained in terms of a slightly increased conformational disorder of the acyl chains. The decreased chain order parameter, S_θ, for DMPC+penetratin confirms this interpretation (Fig. 2). A decreased macroscopic ordering of the DMPC multibilayer stacks caused by the presence of penetratin might also partially explain the observed tendency. However, the IR order parameter of the phosphate and carbonyl bands remain virtually invariant after addition of penetratin (see below), indicating that the peptide only marginally affects the macroscopic arrangement of the lipid bilayer stacks.

On heating the lipid passes the phase sequence gel ($L_{\beta'}$) → ripple gel ($P_{\beta'}$) → liquid crystalline (L_α). In the gel phase the methylene chains exist predominantly in the extended all-*trans* conformation. Their long axes tilt with respect to the membrane normal. The chain order parameter, S_θ, increases upon transformation into the ripple phase whereas $COG(\nu_s(CH_2))$ remains virtually constant. The invariance of the latter parameter indicates that the conformation of the chains only weakly changes at the $L_{\beta'}/P_{\beta'}$ phase transition whereas the tilt angle of the chain long axes decreases as

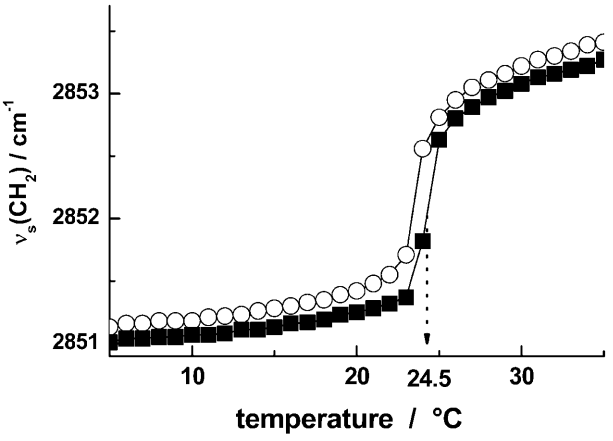

FIGURE 1 Center of gravity of the symmetric methylene stretching vibrational band of fully hydrated DMPC films in the absence and presence of penetratin ($(L/P) = 30$ mol/mol) as a function of temperature.

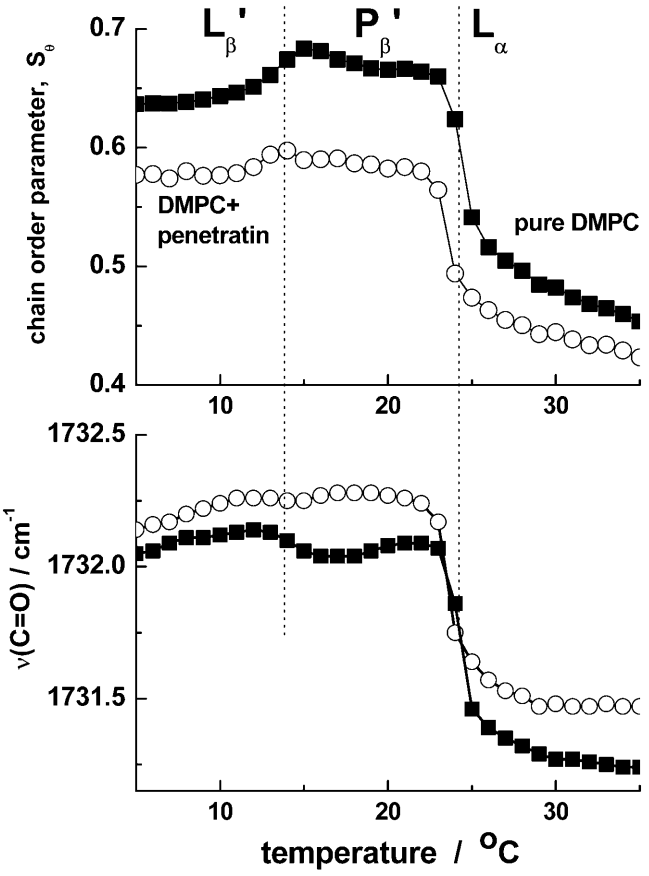

FIGURE 2 Chain order parameter, S_θ (Eq. 2) (*top panel*), and center of gravity of the C=O stretching vibrational band (*bottom panel*) of fully hydrated DMPC films in the absence and presence of penetratin ($(L/P) = 30$ mol/mol) as a function of temperature. The vertical dotted lines indicate the phase transitions of pure DMPC.

indicated by the alteration of the order parameter, S_θ (Fig. 2). The subsequent chain melting transition between the ripple gel and the liquid crystalline phase is characterized by the parallel alterations of COG($\nu_s(CH_2)$) and S_θ. These tendencies reflect the decrease of segmental order owing to the appearance of *gauche* defects. The addition of penetratin induces a systematic downwards shift of S_θ and the partial disappearance of the pretransition. This event is very sensitive to the incorporation of small amounts of additives, which perturb the lipid packing in the gel phase. The effect of penetratin on the discussed infrared parameters, and on the phase behavior of fully hydrated DMPC films, gives clear evidence that the peptide interacts with the membrane. However, its presence only slightly affects the molecular architecture in the hydrocarbon region of the bilayer in the solid and fluid phases.

We also performed DSC measurements on DMPC multilamellar vesicles in the presence and absence of penetratin to prove the phase behavior in diluted aqueous solution (10 mM phosphate buffer, pH 7.4, lipid concentration 5 mM, $(L/P) \approx 10$; multilamellar vesicles were prepared by freeze-thawing). No significant effect of the peptide was detected. This result does not surprise us, because penetratin distributes between the aqueous and membrane phase according to a partition equilibrium. Recently, we showed that penetratin binding to membranes is well described by a surface partitioning model, which takes into account that bound penetratin hampers further peptide binding owing to electrostatic repulsion (Binder and Lindblom, 2003a). The amount of bound peptide strongly depends on the lipid concentration in the sample. For a lipid concentration of 5 mM as in the DSC experiments, <20% of the peptide is expected to associate with the membrane if one uses an intrinsic binding constant of $K_b = 80\ M^{-1}$ (Persson et al., 2003). Hence, the molar ratio of lipid/bound peptide is >50:1 in this case. In the cast films used for the IR measurements each lipid molecule adsorbs ~14–18 water in the saturated water atmosphere (Binder, 2003; Jendrasiak and Hasty, 1974; Kint et al., 1992; Markova et al., 2000). This corresponds to a lipid concentration of ~1–1.5 M. The binding model predicts that nearly all peptide binds to the membranes at these conditions. The partition equilibrium of the peptide in the hydrated films is strongly shifted toward the lipid phase, and thus this technique allows us to study the peptide in the bound state.

Hydration and orientation of the polar groups of DMPC

The center of gravity of the C=O stretching band, ν(C=O), sensitively responds to local hydration effects (Binder, 2003; Blume et al., 1988). For example, the decrease in ν(C=O) at the pretransition and especially at the main phase transition of DMPC upon heating reflects the partial invasion of water into the carbonyl region of the membrane owing to a loosening of the molecular packing of the lipid (Fig. 2). Penetratin induces a systematic shift in ν(C=O) toward higher wavenumbers. The interaction of penetratin with the bilayer is obviously accompanied by the partial dehydration of the carbonyl groups. Note that the samples are hydrated at constant water activity, $\propto$(RH/100%). Hence the water reservoir provides the amount of water which ensures hydration of the sample at the predefined RH value. There is no competition between the lipid and peptide and their hydrophilic groups for a limited amount of water as in samples containing a fixed number of water molecules. Instead the observed shift of the carbonyl band reflects a decreased accessibility of this moiety in the presence of penetratin for water at conditions of constant RH.

The position of several vibrational modes of the phosphate group are suited as markers for evaluating local hydration and interaction properties of these moieties (see, e.g., Binder, 2003, for an overview). The intense antisymmetric stretching mode of the nonesterified oxygens is distorted by overlap with the bending vibration of D_2O near 1200 cm^{-1} at higher hydration degrees. We therefore used the weaker antisymmetric P-$(OC)_2$ stretches near 820 cm^{-1}, which shift toward higher wavenumbers upon progressive hydration (see Fig. 3 *a*). After addition of penetratin the ν_{as}(P-$(OC)_2$) band appears at higher wavenumbers compared with pure DMPC. This spectral shift possibly reflects increased hydrogen bonding and/or specific iterations with cationic species (Binder and Zschörnig, 2002).

The peptide obviously affects the hydration and interactions of the phosphate groups in the opposite way in comparison with its effect on the carbonyl groups. This seems to be a paradox, but similar tendencies were previously observed upon interaction of selected divalent ions with lipids (e.g., Zn_2^+; Binder et al., 2001; Binder and Zschörnig, 2002) and for the respective band positions of lipids with phosphatidylethanolamine (PE; Binder et al., 1997; Binder and Pohle, 2000) and –glycerol (PG, see below) headgroups compared with their analogs with phosphatidylcholine (PC) headgroups. The different hydration and interaction characteristics of the phosphate and carbonyl groups in these systems are caused by the involvement of the phosphate groups into interactions with neighboring lipids or additives via H-bonds and/or Coulombic forces which, on the other hand, partially screen the carbonyl groups from the water, and thus partially dehydrate these moieties (Binder and Pohle, 2000).

The guanidinium group of arginine ($CN_3D_5^+$) and each amino group of lysine (ND_3^+) of penetratin are potential donors for two and one H-bonds with the electronegative oxygens of phosphate groups of the lipid, respectively, which might explain the observed spectral shift. On the other hand, we found no spectral indications of a conformational change of the phosphate groups due to the presence of penetratin. Hence, the suggested interactions are relatively moderate and much weaker than the effect of divalent metal

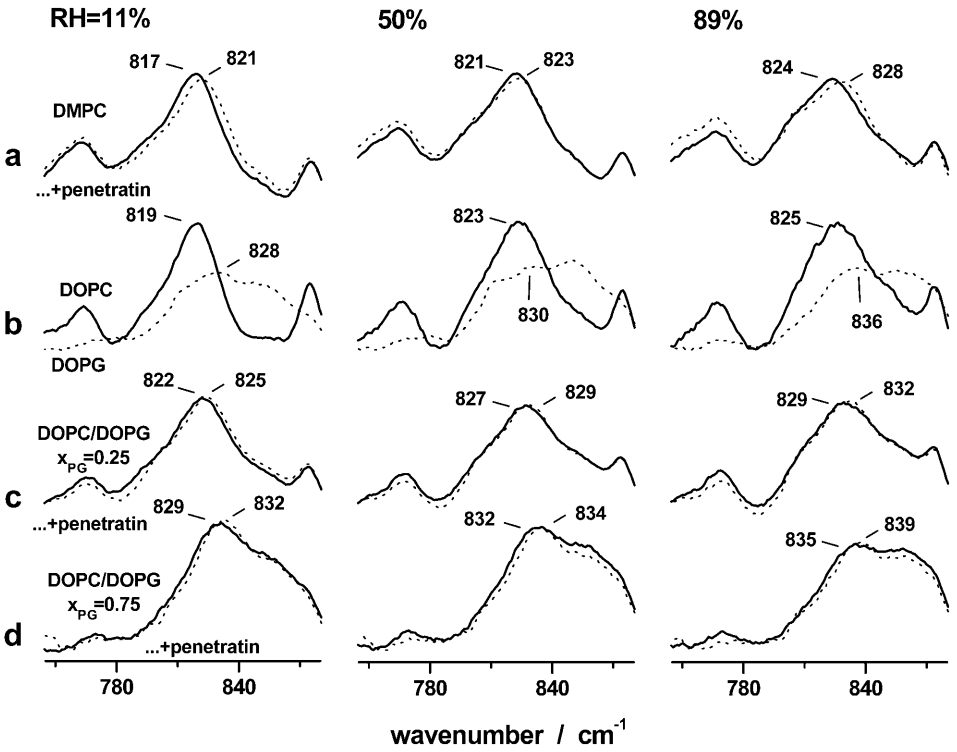

FIGURE 3 Spectral range of the antisymmetric stretching mode of the esterified phosphate oxygens, ν_{as}(P-(OC)$_2$), of DMPC (*a*) and DOPC/DOPG (*c* and *d*) in the presence (*dotted line*) and absence (*full line*) of penetratin at *RH* = 11% (*left*), 50% (*middle*), and 89% (*right*). Panel *b* shows the ν_{as}(P-(OC)$_2$) band of pure DOPC (*full line*) and DOPG (*dotted line*). The maximum positions of the ν_{as}(P-(OC)$_2$) band due to the PC groups are given within the figure in units of cm^{-1}. The right value refers to the respective system with penetratin (molar ratio, (*L*/*P*) = 20–30 mol/mol).

cations, which can induce a measurable rigidification of the phosphate groups (Binder, 2003; Binder and Zschörnig, 2002).

Fig. 4 shows the polarized IR spectra of DMPC membranes in the presence of penetratin ((*L*/*P*) = 30) in the spectral range of the ν(C=O) band of the lipid and of the amide I band of penetratin at low (*RH* = 11%, Fig. 4 *a*) and higher (*RH* = 89%, Fig. 4 *b*) hydration degree. Both spectra show essentially identical features, which also remain unchanged upon further increasing hydration degree up to *RH* = 100% (not shown). Note that the membranes spontaneously assemble into multibilayer stacks, which align parallel on the surface of the ATR crystal. The dichroism of the ν(C=O) band near 1735 cm^{-1} refers to an IR order parameter $S_{IR} \approx -0.2$. It indicates that the C=O bonds orient predominantly parallel with respect to the membrane surface. The dichroic spectrum in the region of the ν(C=O) band clearly shows the existence of at least two sub-bands of different orientation. The right-hand component near 1725 cm^{-1} can be attributed to a population of stronger hydrated carbonyls, the C=O double bonds of which point more parallel to the membrane plane. The C=O bonds of the left-hand component band near 1748 cm^{-1} orient slightly more in the direction of the membrane normal. The bigger wavenumber suggests that the respective carbonyls are only weakly involved into H-bonding.

The mean IR order parameter of the ν(C=O) band and of the selected vibrational modes of the phosphate groups of fully hydrated DMPC in the presence and absence of penetratin do virtually not change at the phase transitions of the lipid as a function of temperature (not shown). Hence, orientation and ordering of the polar part of the lipid are virtually independent of the phase state of the lipid. In addition, no significant effect of penetratin on the mean order of the carbonyl and phosphate groups of the lipid was found.

The amide I and II bands of penetratin: conformation and location of the peptide in the DMPC bilayer

The amide I band of penetratin shows an intense IR band at 1610–1620 cm^{-1}, and a weaker component near 1685 cm^{-1} (Fig. 4). The doublet is typical of an antiparallel β-sheet conformation (Byler and Susi, 1986; Miyazawa, 1960). The relatively small wavenumber of the low frequency component can be attributed to deuteration (see, e.g., Binder et al., 2000), to relatively strong hydrogen bonding and/or a distortion of secondary structure (see Torii and Tasumi, 1996, and references cited therein). The guanidyl group of deuterated arginine leads to antisymmetric and symmetric stretching bands near $\nu_{as}(CN_3D_5^+)_{arg} \approx 1608$ cm^{-1} and $\nu_s(CN_3D_5^+)_{arg} \approx 1586$ cm^{-1} (Chirgadze et al., 1975). The latter band originating from the three arginines per penetratin protrudes as a shoulder in the spectrum of the peptide.

The transition moments of the low and high frequency components of the amide I bands point perpendicular (molecular *x* axis, within the plane of the sheet) and parallel (molecular *z* axis) to the peptide chain axis, respectively. The spectrum of the dichroic ratio, $R(\nu)$, reveals a completely different mean orientation of both transition moments and

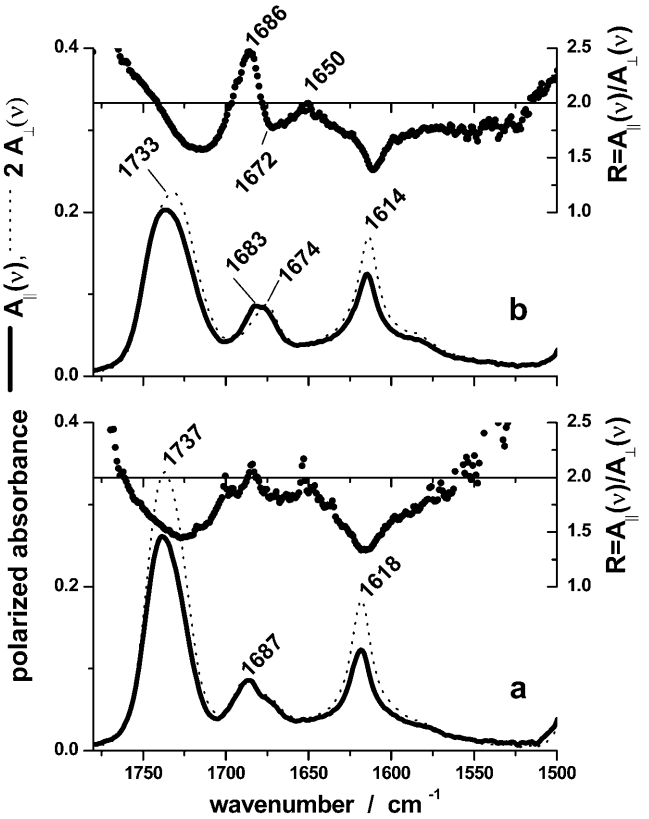

FIGURE 4 Polarized IR spectra, $A_{\parallel}(\nu)$ and $2A_{\perp}(\nu)$, of DMPC in the presence of penetratin ($(L/P) = 30$ mol/mol) at low ($RH = 11\%$, *a*) and higher ($RH = 89\%$, *b*) hydration degree. The lipid exists in the gel (*a*) and in the liquid-crystalline (*b*) state with $R_{W/L} \approx 2$ and 10 adsorbed water molecules per lipid, respectively (see Binder, 2003). The respective spectra of the dichroic ratio, $R(\nu)$, are shown above the absorbance spectra. Note that $R(\nu) = 2.0$ refers $S_{IR} = 0$ (see Eq. 1). Characteristic wavenumbers are shown in units of cm^{-1}. The temperature was $T = 35°C$.

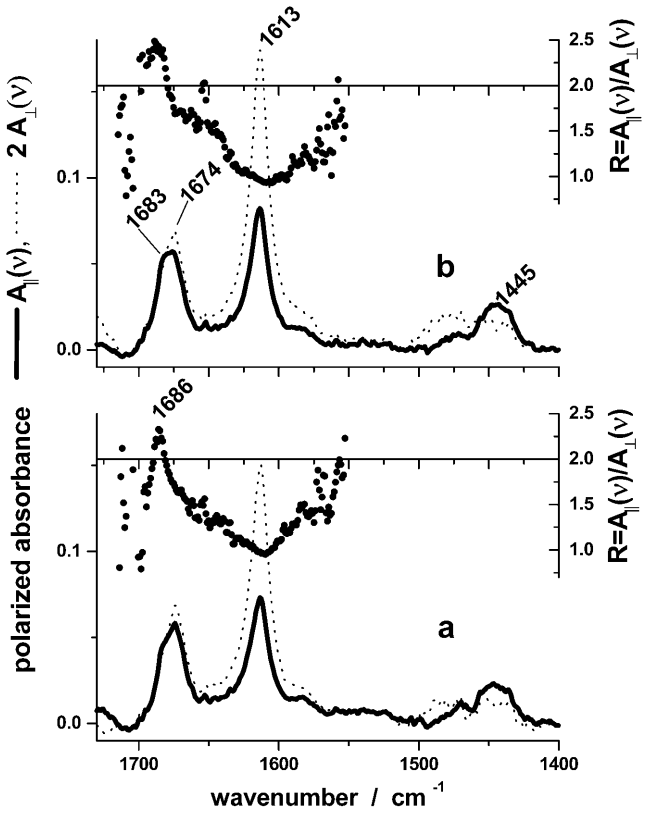

FIGURE 5 Polarized difference spectra, $\Delta A_{\parallel}(\nu) = A_{\parallel}^{L+P}(\nu) - A_{\parallel}^{L}(\nu)$ and $2\Delta A_{\perp}(\nu) = 2A_{\perp}^{L+P}(\nu) - 2A_{\perp}^{L}(\nu)$, where the superscript $L+P$ refers to the spectra of the mixed systems shown in Fig. 4 and the superscript L to the respective pure lipid, respectively. Parts *a* and *b* are recorded at $RH = 11\%$ and 89%, respectively ($T = 35°C$).

thus a marked ordering of penetratin within the bilayer stacks. The dichroic ratio in the range of the right-hand band, $R_{1615}(\nu) < 2$ (i.e., $S_{IR} < 0$), is compatible with an almost perpendicular orientation of the molecular *x* axis with respect to the bilayer normal, **n**, whereas the long molecular *z* axis adopts an oblique orientation with respect to **n** ($R_{1685}(\nu) > 2$ and $S_{IR} > 0$, see Eq. 1).

Fig. 5 shows the difference between the polarized spectra of penetratin in the presence of DMPC and the polarized spectra of pure DMPC. The spectra of both samples were recorded at identical relative humidity and temperature. The difference spectrum thus provides the spectrum of the peptide in the membrane, if one neglects subtle alterations of the spectrum of DMPC owing to peptide-lipid interactions. The amide II band of the deuterated peptide protrudes near 1445 cm^{-1} (Fig. 5). Note that the strong CH_2 bending mode of the lipid chains centered at 1467 cm^{-1} masks this feature in the original spectrum.

In lysine the functional group is linked to the backbone by a relatively long aliphatic spacer with four methylene groups. The bending, wagging, and rocking modes of lysine absorb at $\delta(CH_2)_{lys} \approx 1445$ cm^{-1}, $\gamma_W(CH_2)_{lys} \approx 1325$ cm^{-1}, and $\gamma_r(CH_2)_{lys} \approx 1345$ cm^{-1}, respectively (see Barth, 2000, and references cited therein). The difference spectrum indicates no preferential orientation of the respective transition moments in the spectral ranges of the latter two bands. We therefore conclude that the bending vibration of the lysines does not significantly contribute to the dichroism of the amide II band at 1445 cm^{-1}.

For an antiparallel β-sheet one expects a ratio of the integrated absorbance of the two component bands of $(A_{1615}/A_{1685})_{sheet} \approx 5$–10 (Blaudez et al., 1993; Chirgadze et al., 1975). The respective ratio of penetratin is clearly smaller, at $(A_{1615}/A_{1685})_{exp} \approx 2$–3. One explanation of this discrepancy can be viewed in the existence of a second structural mode, which also absorbs in the spectral region of the weaker sub-band of the antiparallel β-sheet. A previous IR reflection absorption study of mixed penetratin+lipid films at the air-water interface reveals a significant fraction of β-turns ($X_{turn} \approx 0.15$), which adsorb near 1670 cm^{-1} (Bellet-Amalric et al., 2000). For equal molar extinction coefficients of β-sheets and turns one expects a value of the ratio of the absorbance of the low and high frequency band

of $(A_{1615}/A_{1685})_{\text{sheet+turn}} \approx (A_{1615}/A_{1685})_{\text{sheet}}/[1+((A_{1615}/A_{1685})_{\text{sheet}}+1) \times X_{\text{turn}}/(1-X_{\text{turn}})] \approx 2$–$5$ in agreement with our observation. The dichroism spectrum of penetratin reveals that the high frequency amide I band clearly represents the superposition of at least two components of different dichroism centered near 1686 cm^{-1} and 1672 cm^{-1}, respectively (see *upper panel* in Figs. 4 and 5). Hence, the existence of such structural units can explain the relatively strong absorbance of the high-frequency component band of penetratin.

The interpretation of the β-sheet characteristics of the amide I band in terms of a hairpin structure (and/or aggregates, see below) is confirmed by recent fluorescence measurements, which reveal an anomalous decrease in the mean lifetime and intensity of the tryptophan fluorescence of penetratin upon interaction with lipid membranes (Christiaens et al., 2002). This result can be explained by a relatively close approach between the tryptophans and the charged residues in a hairpin structure, e.g., between Trp^{48} and Arg^{52} and Arg^{53} (see Fig. 8 below for illustration) because lysines and arginines are potential quenchers of the tryptophan fluorescence. The twist of the hairpin has been suggested in the middle of the molecule near the Gln-Asp residues (Bellet-Amalric et al., 2000). This assumption is supported by the high propensity of asparagine for turn formation which has been established in different model peptides (Dyson et al., 1988, 1998; Gao et al., 2002; Johnson et al., 1993).

The dichroism of the amide I band is nearly independent of the hydration degree and the phase state of the lipid. Note that DMPC exists in the gel phase at $RH = 11\%$ (Figs. 4 *a* and 5 *a*) and in the liquid crystalline phase at $RH = 89\%$ (Figs. 4 *b* and 5 *b*). Temperature-dependent studies of fully hydrated DMPC+penetratin systems ($RH = 100\%$) provide similar results. Note also that the IR order parameter of the headgroup modes of the lipid is nearly independent of the phase state of DMPC (see above). This result is compatible with the conclusion that penetratin loosely binds to the headgroup region of the bilayer and this way only weakly affects the phase behavior of DMPC.

The localization of penetratin at the polar interface of the membrane is further confirmed by the hydration-dependent shift of the amide I band toward smaller wavenumbers (Figs. 4–6). The difference spectrum shown in Fig. 6 *b* clearly reveals the hydration-induced shifts in terms of a dispersion-like pattern in the range of the C=O band of the lipid and of the two amide I sub-bands of penetratin.

After the exchange of H_2O by D_2O vapor in the sample chamber the amide II band of proteated peptide near 1530 cm^{-1} completely disappears within minutes, and instead, the amide II band of the deuterated peptide appears near 1445 cm^{-1} (see Fig. 5). The spectral shift indicates that the hydrogens are completely replaced by deuterons. Note also that the water associated with the lipid exchanges completely from H_2O to D_2O within minutes. Both the hydration- and isotope-dependent shifts of the amide I and II bands indicate

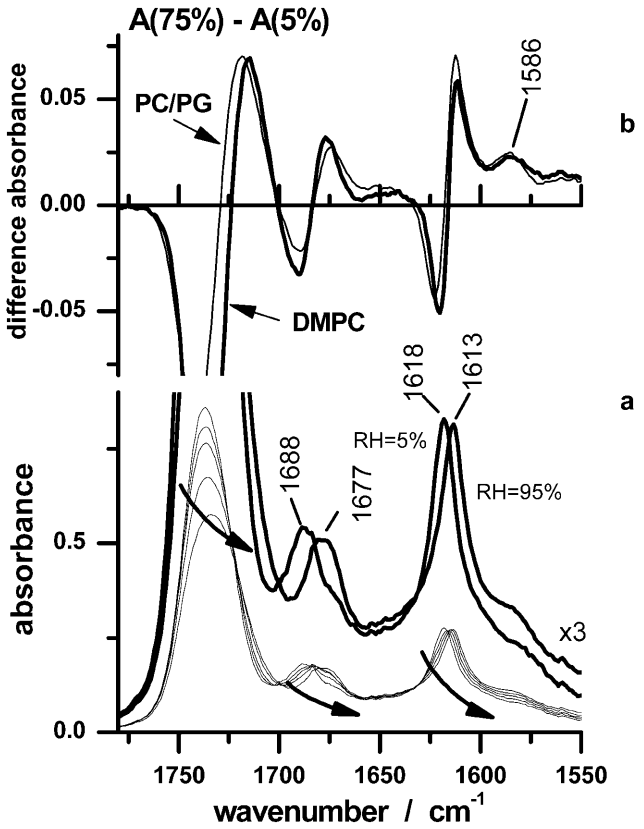

FIGURE 6 Spectral range of the amide I band of penetratin and of the C=O stretching band of DMPC of mixed DMPC/penetratin ($(L/P) \approx 30$ mol/mol) multibilayer stacks as a function of relative humidity, $RH = 5$, 25, 50, 75, and 95%. The spectra of the lowest and highest RH are enlarged. Progressive hydration shifts all displayed bands toward smaller wavenumbers (see *arrows*). Peak positions are given in units of cm^{-1}. The difference spectrum referring to $RH = 75\%$ and 5% amplifies the hydration-induced spectral changes (see *b*, *thick line*). The thin line gives the respective difference spectrum of penetratin in the presence of anionic DOPC/DOPG membranes ($X_{\text{PG}} = 0.75$, PC/PG).

that the C=O and N-H bonds of the peptide are accessible to the water, and thus the peptide is essentially not buried within the hydrophobic core of the bilayer.

The spectrum of the dichroic ratio indicates an additional weak component near 1650 cm^{-1}, which can be assigned to a small fraction of α-helical and/or disordered structures originating, e.g., from peptide bonds that are not involved in secondary structures (Fig. 4). Magzoub and co-workers observed the coexistence of α-helical, β-sheet, and disordered conformations of penetratin in diluted vesicle suspensions (Magzoub et al., 2002). Both the increase of the peptide concentration and the increase in the molar fraction of anionic lipid in the membrane facilitate an $\alpha \rightarrow \beta$-transition of the peptide since the fraction of β-sheets increases, whereas the fraction of α-helices decreases. The correlation between the (L/P) ratio and the occurrence of β-sheets suggests that the formation of the β-structure is related to peptide-peptide interactions, for example by the stacking of penetratin monomers into dimers or oligomers

as has been observed for hydrophobic hexapeptides upon membrane binding (Wimley et al., 1998). Other studies suggest that dimerization is an essential prerequisite for penetratin internalization into cells (Derossi et al., 1994).

On the other hand, the propensity of model peptides for intramolecular hairpin formation was found to depend strongly on the environment, sequence context, and solution properties, and on the peptide concentration in particular, without aggregation of peptide monomers—because inter-peptide interactions induce an initial hydrophobic collapse, which leads to the formation of the turn (Dyson et al., 1988; Silva et al., 1999). Our IR measurements provide no indication of a concentration-dependent $\alpha \rightarrow \beta$ transformation (see also next section). It is, however, important to note that an alternative interpretation of the IR data in terms of an intermolecular antiparallel β-sheet of dimeric penetratin leads to a similar picture as has been suggested for the hairpin structure, namely a plate-like sheet with a heterogeneous distribution of charged and hydrophobic residues along the edges, which obliquely inserts into the headgroup region of the membrane (see also below).

Penetratin in the presence of charged membranes

In our recent calorimetric study we found that upon titration of penetratin to mixed DOPC/DOPG vesicles the peptide first binds to their outer surface (Binder and Lindblom, 2003a). Its binding capacity increases with the content of anionic lipid in the membrane. At a molar fraction of DOPG of $X_{PG} \approx 0.5$ and a molar ratio of lipid/bound peptide of $\sim(L/P) \approx 20$, the membranes become permeable, and after internalization, penetratin also binds to the inner monolayer. The results were rationalized in terms of an electroporation-like mechanism of penetratin permeabilization.

We studied the IR spectrum of penetratin in the presence of mixed DOPC/DOPG membranes with a molar fraction of anionic DOPG of $X_{PG} = 0.25$ and 0.75 as a function of the hydration degree in a D_2O atmosphere to estimate the effect of surface charge of the membranes on the secondary structure of the peptide. In a second series of experiments we increased the molar ratio lipid/peptide (L/P) from $\sim$7 to $\sim$150 (Fig. 7). These conditions include the concentration ranges corresponding to impermeable (e.g., $X_{PG} = 0.25$) and permeable (e.g., $X_{PG} = 0.75$ and $(L/P) = 7$) vesicles (see above).

The β-sheet characteristics of the amide I band remains almost unchanged in all experiments and shows essentially the same dichroism and shape independently of X_{PG} (not shown) and (L/P) (Fig. 7) as in the presence of DMPC. Note that each sample remained at minimum 30 h in the sample chamber. No time-dependent spectral changes were observed.

The ν_{as}(P-(OC)$_2$ band of pure DOPG is considerably broader and shifts toward higher wavenumbers compared

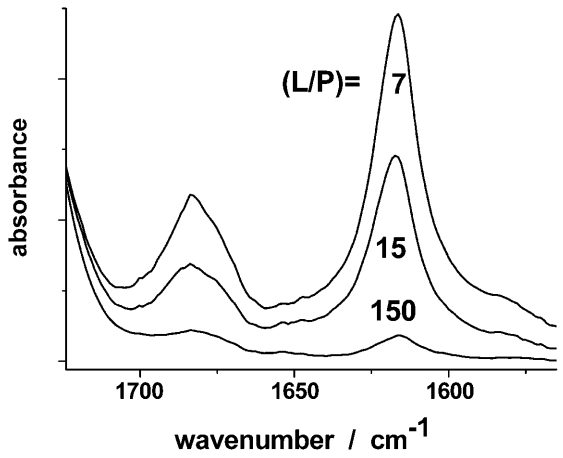

FIGURE 7 Spectral range of the amide I band of penetratin in the presence of mixed DOPC/DOPG multibilayer stacks of a molar fraction of anionic DOPG of $X_{PG} = 0.75$ ($T = 25°C$ and $RH = 25\%$). The lipid/peptide molar ratio was increased from $(L/P) = 7$ to 150 mol/mol (see figure). The signature of an antiparallel β-sheet is evident in all spectra.

with its width and position in DOPC (see Fig. 3 *b*). These differences can be interpreted in terms of an altered conformation of the C-O-P-O-C backbone of the PG headgroup and of additional H-bonds between the esterified oxygens of the phosphate group and the –OH groups of DOPG.

The maximum position of the phosphate band of the PC headgroups shifts toward higher wavenumbers in the mixed DOPC/DOPG membrane with increasing fraction of DOPG, presumably because the $-$OH groups of DOPG serve as additional donors for H-bonds with the phosphate groups (Fig. 3, *c* and *d*). The shift slightly but systematically increases after addition of penetratin. We suggest the formation of additional H-bond to the $-ND_3^+$ and $-CN_3D_5^+$ moieties of penetratin as in the case of DMPC (see above). On the other hand, the effect of penetratin on the C=O stretching mode decreases in the anionic membranes (see Fig. 6 *b*) and virtually disappears at $X_{PG} = 0.75$. A penetratin-induced downwards shift of this mode, as an indication of the invasion of water into the region of carbonyl groups and/or enhanced H-bonding to additives, was not observed.

Comparison of the difference spectra of hydrated DMPC and DOPC/DOPG ($X_{PG} = 0.75$) samples show similar shifts of the amide I sub-bands indicating a similar water accessibility of penetratin if bound to zwitterionic and anionic membranes (see Fig. 6 *b*). The carbonyl band of the DOPC/DOPG mixture is clearly blue-shifted at the raising flank compared with DMPC owing to the weaker hydration of the carbonyls (see above). Interestingly, the absorbance of a small peak increases in the range of the $\nu_s(CN_3D_5^+)_{arg}$ mode near 1586 cm^{-1} upon progressive hydration. We suggest that this effect is caused by the hydration of the guanidyl moieties of the side chains of the arginines.

Orientation of membrane-bound penetratin

Let us analyze the orientation of penetratin in terms of the hairpin structure illustrated in Fig. 8. The dichroic ratio, $R = A_{\parallel}/A_{\perp}$, of the high- and low-frequency bands with transition moments pointing along the peptide chain (z axis) and along the intramolecular H-bonds (x axis) were obtained from the integrated band intensities of the polarized difference spectra after band separation and baseline correction (see Fig. 5 and Eq. 1). Table 1 summarizes the IR order parameters and the mean orientation angles of the antiparallel β-sheet, which lies within the x–z plane of the molecular frame of reference (Fig. 8). The transverse molecular x axis aligns essentially parallel to the membrane surface, whereas the longitudinal z axis orients in an oblique fashion according to this analysis.

Note that the mean orientation angle $\langle\theta\rangle$ provides only a rough impression of the real orientation of the respective transition moment in the membrane. It yields adequate results if the distribution of the tilt angle is limited to a relatively narrow angular range. There is considerable uncertainty in the order parameter of the high frequency mode owing to its smaller absorbance and its overlap with neighboring absorption bands. Hence, the infrared order parameter of the band near 1680 cm^{-1} reflects an orientation of the long molecular axis which, on the average, slightly deviates from the random value ($S_{IR} = 0$, corresponding to $\langle\theta\rangle = 55°$) toward $S_{IR} > 0$ (and $\langle\theta\rangle < 55°$).

Selective quenching of the tryptophans by water-soluble acrylamine indicates that Trp^{48} is inserted more deeply into the lipid bilayer than Trp^{56} (Christiaens et al., 2002). This interpretation presumes an oblique orientation of the molecular x axis and/or z axis with respect to the membrane plane. Consideration of the dichroism data leads to the conclusion that, on the average, the turn is more deeply inserted into the membrane than the terminal part because Trp^{48} is located closer to the turn than Trp^{56} (see Fig. 8).

The amino acid sequence and membrane binding of penetratin

Fig. 9 illustrates the distribution of positive charges, and of the residue free energy of transfer from the aqueous into the membrane phase along the peptide sequence. The first half part of the peptide (i.e., residues 43–50; the numbers refer to the position of the residues in the *Antennapedia* homeodomain) carries only two nominal charges in contrast to the second half (i.e., residues 51–58) with five charged groups. The cumulative residue free energy is −2.7 kJ/mole for the first half and +10.2 kJ/mole for the second half using the single residue values (White and Wimley, 1998; see also Fig. 9, this article). Note that positive values refer to a loss of free energy, and thus to a preference for the aqueous phase and vice versa. On the other hand, if one cuts the hypothetical hairpin perpendicularly to the long edges, the terminal part (residues 43–46 and 55–58) possesses six charges and a cumulative transfer free energy of +13.3 kJ/mole contrarily to the part near the turn (residues 47–54) with two charges and a transfer free energy of −5.8 kJ/mole. Hence, the two long ''edges'' of the hairpin conformation on the one hand and their terminal part and the turn on the other hand differ considerably in charge and preference for membrane binding. The heterogeneous distribution of charged and hydrophobic residues implies an oblique orientation of the peptide, where the more hydrophobic part near the turn is located closer to the membrane and the more hydrophilic terminal part faces toward the aqueous phase (see Fig. 8). Note that this insertion mode also realizes a localization of the C=O moieties of the asparagine and glutamine side chains forming the turn in the vicinity of the lipid carbonyl groups, and thus in a region of intermediate polarity.

The charge distribution along the hairpin lets us further suggest a preferential location of the peptide at the polar interface of the membrane in such a way that the

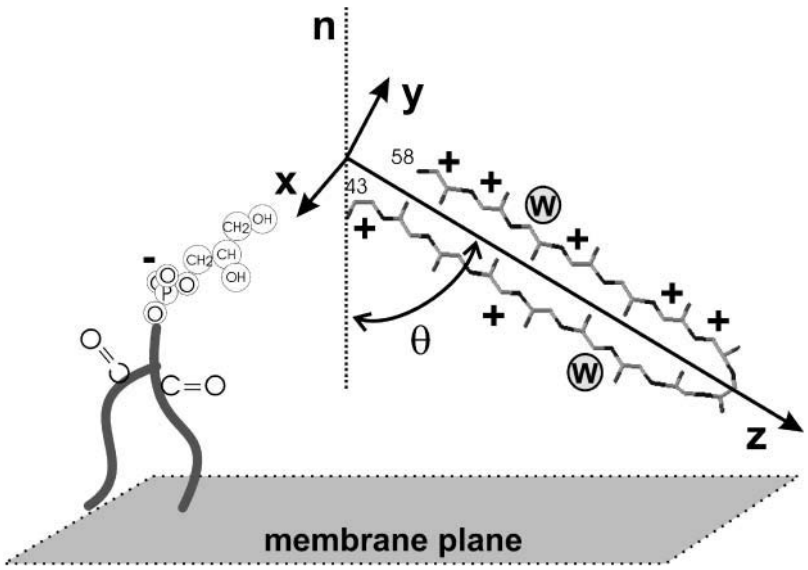

FIGURE 8 Hairpin conformation of penetratin formed by an antiparallel β-sheet and a turn as proposed by Bellet-Amalric et al. (2000). The transition moments of the amide I band components of the antiparallel β-sheet centered near 1615 cm^{-1} and 1685 cm^{-1} orient along the molecular z and x axes, respectively (see also Table 1). The left panel shows an anionic DOPG molecule. The plane is oriented parallel to the membrane surface.

TABLE 1 Orientation of the hairpin conformation of penetratin at the polar interface of DMPC membranes

Molecular axis	Mode	IR order parameter, S_{IR}	Mean orientation angle relative to the membrane normal, $\langle\theta\rangle$, deg*
x, along the H-bonds	1610–1620	$S_x = -0.3 \pm 0.03$	$\langle\theta_x\rangle > 68$
y, perpendicular to the plane of the sheet		$S_y = +0.1^{\dagger}$	$\langle\theta_y\rangle < 51$
z, along the peptide chain	1680–1690	$S_z = +0.2 \pm 0.06$	$\langle\theta_z\rangle < 47$

DMPC:penetratin = 30:1 mol/mol, $RH = 89\%$, and $T = 35°C$; see Fig. 5 *b*.
*The mean angles are calculated according to $\langle\theta_{\mu n}\rangle \approx \arccos\left(\sqrt{1/3 \times (2S_{IR} + 1)}\right)$. The values represent maximum and minimum estimates for $\theta < 55°$ and $\theta > 55°$, respectively (see text and Binder et al., 2000, for details).
$^{\dagger}S_y = -(S_x + S_z)$, see Binder and Schmiedel (1999).

sixfold-charged terminal part of the hairpin orients toward the anionic phosphate groups of the lipid. The functional groups of lysine and arginine are linked to the backbone by relatively long aliphatic spacers of four and three methylene groups, respectively. Hence, the charged groups are relatively flexible to optimize their position with respect to the anionic phosphates of the surrounding lipids.

It has been found that the cell uptake of penetratin analogs is related to their lipid-binding affinity and requires a minimal hydrophobicity and net charge (Drin et al., 2001b). On the other hand, specific interactions such as the ability of the arginines to form two H-bonds per residue (see Henry and Washington, 2003, and references cited therein) and/or the high propensity of aromatic tryptophans to accumulate in the interfacial region of the membrane (Killian et al., 1996; Schulz, 1994; Yau et al., 1998) seem to be of great importance for membrane-penetratin interactions. It has been shown in several studies that the transfection efficiency of model peptides is related to the presence of tryptophan and/or arginines in their sequences (Derossi et al., 1996, 1994; Dunican and Doherty, 2001; Henry and Washington, 2003; Lindgren et al., 2000; Putnam et al., 2001; Schwarze and Dowdy, 2000).

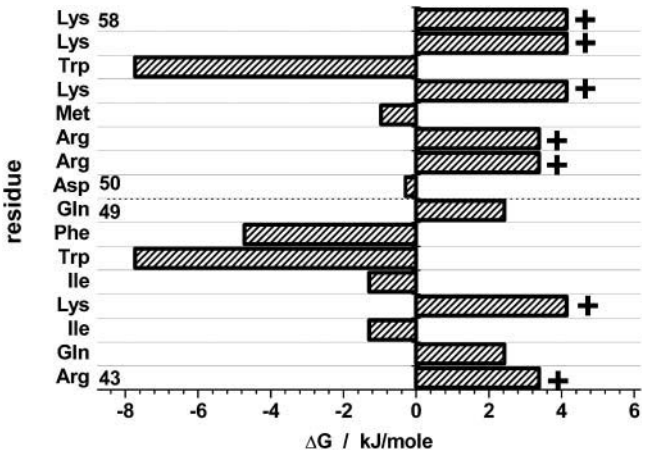

FIGURE 9 Single residue free energy of transfer from the water into the membrane phase according to White and Whimley (1998) for penetratin. Cationic residues are indicated by +. The horizontal dotted line indicates the tentative position of the turn at which the peptide backbone is suggested to fold back into the hairpin conformation. The numbers 43–58 refer to the position of the residues in the homeodomain of *Antennapedia*.

As such, it appears that the sequence of penetratin requires the asymmetric distribution of positively charged arginines juxtaposed with the aromatic residues. Possibly the anchoring of tryptophans in the glycerol region of the lipid and/or H-bonds between the arginines and the phosphate groups stabilize the orientation and location of penetratin at the membrane surface. As a consequence the electrostatic potential produced by the peptide increases due to ''image'' charge effects and because of the decreased dielectric constant near the membrane (S. McLaughlin, personal communication, 2003) enabling the effective mutual compensation of lipid and peptide charges.

The relatively high positive charge of cell-penetrating peptides suggests a mechanism of membrane permeabilization, which is based mainly on electrostatic interactions. Our previous isothermal titration calorimetry results indicate that an increasing amount of bound penetratin progressively neutralizes the lipid charges in the outer monolayer. This trend destabilizes the bilayer structure and this way facilitates the translocation of the peptide through the membrane (Binder and Lindblom, 2003a). The oblique orientation of penetratin β-sheets in the interfacial region of the membrane ensures a close approach between the cationic side chains of the peptide and the anionic phosphate groups of the surrounding lipids. The coverage of the outer membrane surface by penetratin β-hairpins enables the effective mutual compensation of positive and negative charges as one prerequisite for the onset of the electroporation-like permeabilization of the bilayer as suggested before (Binder and Lindblom, 2003a).

SUMMARY AND CONCLUSIONS

Infrared spectra of penetratin in the presence of zwitterionic and anionic lipid membranes show the characteristics of an antiparallel β-sheet with a small fraction of turns. This result confirms the interpretation of the structure of penetratin in terms of a hairpin conformation proposed previously (Bellet-Amalric et al., 2000). Visualizing the hairpin as a ladder, whose rungs correspond to the interstrand hydrogen bonds, the linear dichroism of the amide I band supports a model, in which the rungs are almost parallel with the membrane surface, and the long axis of the ladder orients in an oblique fashion with respect to the surface.

The nearly unaffected phase behavior of DMPC in the presence of penetratin indicates that the peptide superficially

binds to the polar region of the membrane and does not penetrate into the hydrophobic core of the bilayer. The existence of specific bindings, like H-bonds between the $-ND_3^+$ and $-CN_3D_5^+$ end groups of the lysine, and especially arginine side chains and the electronegative oxygens of the phosphate groups, have been concluded from characteristic shifts of vibrational modes of the phosphate groups after addition of penetratin. This effect is accompanied by the partial dehydration of the carbonyls of zwitterionic DMPC, possibly because the adsorbed peptide screens the C=O groups from the aqueous phase.

As such, it appears that the hairpin structure of penetratin provides an asymmetric distribution of positively charged arginines and lysines juxtaposed with the tryptophan residues, which enable the anchoring of the peptide in the polar part of the membranes and the effective interaction with the anionic lipid charges. The mutual charge compensation was indeed observed in our previous calorimetric experiments. We proposed an electroporation-like mechanism of penetratin internalization according to which the asymmetric compensation of lipid charges by bound peptide destabilizes the bilayer architecture by electrostatic effects, and in this way enables translocation of the peptide through the bilayer. The molecular mechanism of the permeation step is unknown. On one side, inversely curved lipid structures can be assumed to mediate permeation of the peptide through the hydrophobic core of the bilayer; however, on the other side, the uneven distribution of hydrophobic and polar residues along the hairpin might facilitate flip-flop events of the peptide through the destabilized membrane. Thus, the determinants for internalization of penetratin appear to be a peptide sequence of 16 amino acids with a distribution of positively charged residues, and possibly also of aromatic tryptophans, along a β-sheet conformation.

REFERENCES

Barth, A. 2000. The infrared absorption of amino acid side chains. *Prog. Biophys. Mol. Biol.* 74:141–173.

Bellet-Amalric, E., D. Blaudez, B. Desbat, F. Graner, F. Gauthier, and A. Renault. 2000. Interaction of the third helix of *Antennapedia* homeodomain and a phospholipid monolayer, studied by ellipsometry and PM-IRRAS at the air-water interface. *Biochim. Biophys. Acta.* 1467:131–143.

Berlose, J. P., O. Convert, D. Derossi, A. Brunissen, and G. Chaissaing. 1996. Conformational and associative behavior of the third helix of *Antennapedia* homeodomain in membrane-mimetic environment. *Eur. J. Biochem.* 242:372–386.

Binder, H. 2003. The molecular architecture of lipid membranes—new insights from hydration-tuning infrared linear dichroism spectroscopy. *Appl. Spectrosc. Rev.* 38:15–69.

Binder, H., A. Anikin, B. Kohlstrunk, and G. Klose. 1997. Hydration-induced gel states of the dienic lipid 1,2-Bis(2,4-octadecanoyl)-*sn*-glycero-3-phosphorylcholine and their characterization using infrared spectroscopy. *J. Phys. Chem. B.* 101:6618–6628.

Binder, H., K. Arnold, A. S. Ulrich, and O. Zschörnig. 2000. The effect of Zn^{2+} on the secondary structure of a histidine-rich fusogenic peptide and its interaction with lipid membranes. *Biochim. Biophys. Acta.* 1468:345–358.

Binder, H., K. Arnold, A. S. Ulrich, and O. Zschörnig. 2001. Interaction of Zn^{2+} with phospholipid membranes. *Biophys. Chem.* 90:57–74.

Binder, H., and K. Gawrisch. 2001. Effect of unsaturated lipid chains on dimensions, molecular order and hydration of membranes. *J. Phys. Chem. B.* 105:12378–12390.

Binder, H., and G. Lindblom. 2003a. Charge-dependent translocation of the Trojan peptide penetratin across lipid membranes. *Biophys. J.* 85: 982–995.

Binder, H., and G. Lindblom. 2003b. Interaction of the Trojan peptide penetratin with anionic lipid membranes—a calorimetric study. *Phys. Chem. Chem. Phys.* 5:5108–5117.

Binder, H., and W. Pohle. 2000. Structural aspects of lyotropic solvation-induced transitions in phosphatidylcholine and phosphatidylethanolamine assemblies revealed by infrared spectroscopy. *J. Phys. Chem. B.* 104:12039–12048.

Binder, H., and H. Schmiedel. 1999. Infrared dichroism investigations on the acyl chain ordering in lamellar structures. I. The formalism and its application to polycrystalline stearic acid. *Vibrational Spectrosc.* 21: 51–73.

Binder, H., and O. Zschörnig. 2002. The effect of metal cations on the phase behavior and hydration characteristics of phospholipid membranes. *Chem. Phys. Lipids.* 115:39–61.

Blaudez, D., T. Buffeteau, J. C. Cornut, B. Desbat, N. Escafre, M. Pezolet, and J. M. Turlet. 1993. *Appl. Spectrosc.* 47:869–874.

Blume, A., W. Hübner, and G. Messner. 1988. Fourier transform infrared spectroscopy of ^{13}C=O-labeled phospholipids. Hydrogen bonding to carbonyl groups. *Biochemistry.* 27:8239–8249.

Byler, D. M., and H. Susi. 1986. Examination of the secondary structure of proteins by deconvolved FTIR spectra. *Biopolymers.* 25:469–487.

Chirgadze, Y. N., O. V. Federov, and N. P. Trushina. 1975. Estimation of amino acid residue side chain absorption in the infrared spectra of protein solution in heavy water. *Biopolymers.* 14:679–694.

Christiaens, B., S. Symoens, S. Vanderheyden, Y. Engelborghs, A. Joliot, A. Prochiantz, J. Vanderkerckhove, M. Rosseneu, and B. Vanloo. 2002. Tryptophan fluorescence study of the interaction of penetratin peptides with model membranes. *Eur. J. Biochem.* 269:2918–2926.

Czajlik, A., E. Mesko, B. Penke, and A. Perczel. 2002. Investigation of penetratin peptides. Part 1. The environment-dependent conformational properties of penetratin and two of its derivatives. *J. Pept. Sci.* 8:151–171.

Derossi, D., S. Calvet, A. Trembleau, A. Brunissen, G. Chassaing, and A. Prochiantz. 1996. Cell internalization of the third helix of the *Antennapaedia* homeodomain is receptor-independent. *J. Biol. Chem.* 271:18188–18193.

Derossi, D., A. H. Joliot, G. Chassaing, and A. Prochiantz. 1994. The third helix of the *Antennapedia* homodomain translocates through biological membranes. *J. Biol. Chem.* 269:10444–10450.

Drin, G., H. Demene, J. Temsamani, and R. Brasseur. 2001a. Translocation of the pAntp peptide and its amphipathic analogue AP-2AL. *Biochemistry.* 40:1824–1834.

Drin, G., M. Mazel, P. Clair, D. Mathieu, M. Kaczorek, and J. Temsamani. 2001b. Physico-chemical requirements for cellular uptake of pAntp peptide. Role of lipid-binding affinity. *Eur. J. Biochem.* 268:1304–1314.

Dunican, D. J., and P. Doherty. 2001. Designing cell-permeant phosphopeptides to modulate intracellular signaling pathways. *Biopolymers.* 60:45–60.

Dyson, H. J., M. Rance, R. A. Houghten, R. A. Lerner, and P. E. Wright. 1988. Folding of immunogenic peptide fragments of proteins in water solution. I. Sequence requirements for the formation of a reverse turn. *J. Mol. Biol.* 201:161–200.

Dyson, H. J., M. Rance, R. A. Houghten, R. A. Lerner, and P. E. Wright. 1998. Sequence requirements for stabilization of a peptide reverse turn in water solution-proline is not essential for stability. *Eur. J. Biochem.* 255:462–471.

Fragneto, G., F. Graner, T. Charitat, P. Dubos, and E. Bellet-Amalric. 2000. Interaction of the third helix of *Antennapedia* homeodomain with

a deposited phospholipid bilayer: a neutron reflectivity structural study. *Langmuir*. 16:4581–4588.

Gao, F., Y. Wang, Y. Qiu, Y. Li, Y. Sha, L. Lai, and H. Wu. 2002. Beta-turn formation by a six-residue linear peptide in solution. *J. Pept. Res.* 60:75–80.

Hällbrink, M., A. Floren, A. Eomquist, M. Pooga, T. Bartfai, and Ü. Langel. 2001. Cargo delivery kinetics of cell-penetrating peptides. *Biochim. Biophys. Acta.* 1515:101–109.

Harrick, N. J. 1967. Internal Reflection Spectroscopy. Wiley, New York.

Henry, C. M., and C. E. Washington. 2003. Breaching barriers—protein transduction and similar methods are promising techniques for delivering a wide variety of drugs directly into cell. *Chem. Eng. News.* 81:35–43.

Jendrasiak, G. L., and J. H. Hasty. 1974. The hydration of phospholipids. *Biochim. Biophys. Acta.* 337:79–91.

Johnson, W. C. J., T. G. Pagano, C. T. Basson, J. A. Madri, P. Gooley, and I. M. Armitage. 1993. Biologically active Arg-Gly-Asp oligopeptides assume a type II β-turn in solution. *Biochemistry.* 32:268–273.

Killian, J. A., I. Salemink, M. R. R. de Planque, G. Lindblom, R. E. Koeppe, and D. V. Greathouse. 1996. Induction of nonbilayer structures in diacylphosphatidylcholine model membranes by transmembrane *r*-helical peptides: importance of hydrophobic mismatch and proposed role of tryptophans. *Biochemistry.* 35:1037–1045.

Kint, S., P. H. Wermer, and J. R. Scherer. 1992. Raman spectra of hydrated phospholipid bilayers. 2. Water and head-group interactions. *J. Phys. Chem.* 96:446–452.

Ladokhin, A. S., and S. White. 2001. ''Detergent-like'' permeabilization of anionic vesicles by melittin. *Biochim. Biophys. Acta.* 1514:253–260.

Lindberg, M., and A. Gräslund. 2001. The position of the cell-penetrating peptide penetratin in SDS micelles determined by NMR. *FEBS Lett.* 497:39–44.

Lindgren, M., X. Gallet, U. Soomets, M. Hällbrink, E. Brakenhielm, M. Pooga, R. Brasseur, and U. Langel. 2000. Translocation properties of novel cell penetrating transportan and penetratin analogues. *Bioconjugate Chem.* 11:619–626.

Magzoub, M., L. E. Erikson, and A. Gräslund. 2002. Conformational states of the cell-penetrating peptide penetratin when interacting with phospholipid vesicles: effects of surface charge and peptide concentration. *Biochim. Biophys. Acta.* 1563:53–63.

Magzoub, M., K. Kilk, L. E. Erikson, Ü. Langel, and A. Gräslund. 2001. Interaction and structure induction of cell-penetrating peptides in the presence of phospholipid vesicles. *Biochim. Biophys. Acta.* 1512: 77–89.

Markova, N., E. Sparr, L. Wadsö, and H. Wennerström. 2000. A calorimetric study of phospholipid hydration. Simultaneous monitoring of enthalpy and free energy. *J. Phys. Chem. B.* 104:8053–8060.

Mitchell, D. J., D. T. Kim, L. Steinman, C. G. Fathman, and J. B. Rothbard. 2000. Polyarginine enters cells more efficiently than other polycationic homopolymers. *J. Pept. Res.* 56:318–325.

Miyazawa, T. 1960. Perturbation treatment of the characteristic vibrations of polypeptide chains in various configurations. *J. Chem. Phys.* 32: 1647–1652.

Persson, D., P. E. G. Thoren, M. Herner, P. Lincoln, and B. Norden. 2003. Application of a novel analysis to measure the binding of the membrane-translocating peptide penetratin to negatively charged liposomes. *Biochemistry.* 42:421–429.

Persson, D., P. E. G. Thoren, and B. Norden. 2001. Penetratin-induced aggregation and subsequent dissociation of negatively charged phospholipid vesicles. *FEBS Lett.* 505:307–312.

Pooga, M., U. Soomets, M. Hällbrink, A. Valkna, K. Saar, K. Rezai, U. Kahl, J. Hao, X. Xu, Z. Wiesenfeld-Hallin, T. Hokfelt, T. Bartfai, and U. Langel. 1998. Cell penetrating PNA constructs regulate galanin receptor levels and modify pain transmission in vivo. *Nat. Biotechnol.* 16:857–861.

Prochiantz, A. 1996. Getting hydrophilic compounds into cells: lessons from homeopeptides. *Curr. Opin. Neurobiol.* 6:629–634.

Putnam, D., C. A. Gentry, D. W. Pack, and R. Langer. 2001. Polymer-based gene delivery with low cytotoxicity by a unique balance of side-chain termini. *Proc. Natl. Acad. Sci. USA.* 98:1200–1205.

Rothbard, J. B., E. Kreider, and C. L. Van Deusan. W. L., B. L. Wylie, and W. P.A.2002. Arginine-rich molecular transporters for drug delivery: the role of backbone and side-chain variations on cellular uptake. *In* Handbook of Cell-Penetrating Peptides. CRC Press, Boca Raton, FL.

Salamon, Z., G. Lindblom, and G. Tollin. 2003. Plasmon-waveguide resonance and impedance spectroscopy studies of the interaction between penetratin and supported lipid bilayer membranes. *Biophys. J.* 84:1796–1807.

Schulz, G. E. 1994. Bacterial cell wall. *New Compr. Biochem.* 27:343–352.

Schwarze, S. R., and S. F. Dowdy. 2000. In vivo protein transduction: intracellular delivery of biologically active proteins, compounds and DNA. *Trends Pharmacol. Sci.* 21:45–48.

Silva, R. A. G. D., S. A. Sherman, and T. A. Keiderling. 1999. β-Hairpin stabilization in a 28-residue peptide derived from the B-subunit sequence of human chorionic gonadotropin hormone. *Biopolymers.* 50:413–423.

Thoren, P. E. G., D. Persson, M. Karlsson, and B. Norden. 2000. The *Antennapedia* peptide penetratin translocates across lipid bilayers—the first direct observation. *FEBS Lett.* 482:265–268.

Torii, H., and M. Tasumi. 1996. Theoretical analyses of the amide I infrared bands of globular proteins. *In* Infrared Spectroscopy of Biomolecules. H. H. H. Mantsch and D. Chapman, editors. Wiley & Sons, New York. 1–18.

White, S. H., and W. C. Wimley. 1998. Hydrophobic interactions of peptides with membrane interfaces. *Biochim. Biophys. Acta.* 1376:339–352.

Wimley, W. C., K. Hristova, A. S. Ladokhin, L. Silvestro, P. H. Axelsen, and S. White. 1998. Folding of β-sheet membrane proteins: a hydrophobic hexapeptide model. *J. Mol. Biol.* 277:1091–1110.

Yau, W.-M., W. C. Wimley, K. Gawrisch, and S. H. White. 1998. The preference of tryptophan for membrane interfaces. *Biochemistry.* 37:14713–14718.